Gyancity Journal of Electronics and Computer Science,
Vol.6, No.1, pp. 1-10, March 2021
ISSN: 2446-2918 DOI: 10.21058/gjecs.20201.61001

Performance Prediction of SiOC on Insulator based PICs

Ameet Kumar*, Abi Waqas, Faisal Memon, Umair Ahmed Korai

*Electronics Engineering Department
aklanghani@gmail.com

Abstract

In this emerging world of Photonics Silicon oxycarbide (SiOC) is introduced as a platform that has a wide range of tunable refractive indexes that possess very low absorption coefficients. Its physical properties likewise (Optical) and chemical properties can be altered over a large scale in different applications through its composition. In this manuscript, the results obtained using waveguides and directional couplers by multiple simulations that relied on the SiOC technology. In this paper, most simplified design of the coupling coefficient in a certain defined range of width, gap as well as coupling length is proposed. The directional coupler and the waveguide building block's mathematical models are parameterized. In our defined model, the passive devices will be exploited in available circuit simulators used commercially for the stochastic and circuit simulations scheme for SiOC based photonic circuits.

Keywords: *Photonics, SiOC, Circuit Simulation, Building Blocks, Stochastic Analysis*

1. Introduction

The Devices with amplify functionalities in the field of Photonics will be perceived from few building blocks likewise, waveguides, polarizers, multi directional coupling, so forth, to regulate the foundational possessions of sunshine that comprise polarization, phase, and amplitude. These BB'S change a good scope of functionalities and their amalgamation may well be accustomed to accomplish optical signal process. The integrational method allows for the assembly of a variety of common devices with integrated specialties. During this procedure, a systematic and logical set is generated that is responsive to variants that are included within the procedure design kit (PDK), a section of integration tests that will be included in an exceedingly simulation and hold an enormous range of important fabricator layout

information, Design laws, simulation conditions, measurements taken, and so on.) [1–5] In comparison, it gives you the compact statistical formulas you need for circuit experiments. As a consequence, engineers will be using the PDK building block to emulate, test, and refine a circuit in an exceedingly system. By specifically connecting BBs in phase, more traditional integrated optical circuits (PICs) will be developed. The magnetism analysis is no longer needed if the Building blocks are within the specific limitation and the simulation command specified in PDK is followed. The circuit would generate a constant degree of precession, removing the need for an electromagnetic analysis. Circuit and electromagnetic simulations will obtain the same degree of precision when estimating the realization can design circuits concentrating on practical activity and its impression on performance of the system using circuit simulators, exempting technical difficulties and accelerating up the development process [4], [5]. This software approach has been used to recognize complex photonic circuits on a variety of platforms, different substances [1, 2, 6, 7]. To the best of knowledge, the information about how to make with an original material that has recently been seen in advanced photonics for multiple purposes. It is being used in an array of applicants, likewise an substantial for Lithium-ion batteries, For interparticle dielectric materials [8]–[10], photoluminescence [11]–[15], and electroluminescence [14], small optical material is used. Various sampling strategies were used to build SiOC thin films under numerous pre- and post-deposition circumstances [11]–[15]. SiOC technique for advanced photonics was developed in previous projects [16]. To something like the state of the art, the data to process BBs which can also be used for perform circuitry reenactments isn't recorded for within the literature. Much farther, the spectral activity for SiOC in photonics machines with wavelength around 1550 nm or n = 2.2 were observed to be there in the order of 10-4 RIU °C- it is represented among the die-electric platform likewise (SiO2) silica, It has been the most widely reported among die-electric frameworks, include silica (SiO2), silicon oxynitride (SiON), and silicon nitride (SiN) (Si3N4) It enhanced its glass carafe optic co-efficient with an array of all its SiOC waveguides throughout the numerous boundary conditions quantitative approaches and also the thermos adaptive output in all electromagnetic devices The successful refractive index and the band index have also been identified. In the multiple dimensions, the band index measured throughout the SiOC waveguides listed (n = 2.2 at = 1550nm) evenly correlated their measurements, besides that, a SiOC dimensional coupler has also been designed, described, and manufactured utilizing SiOC technique. In its most simplified model, the coupling rate can be determined utilizing various waveguide widths and separating ratios, and also coupling distance and length and width within the same specified range. Such patterns throughout the PICs are indeed the consequence of deterministic modeling.

2. Designing and Experimental Validation of Passive

Gyancity Journal of Electronics and Computer Science,
Vol.6, No.1, pp. 1-10, March 2021
ISSN: 2446-2918 DOI: 10.21058/gjecs.20201.61001

This segment discusses the fabrication of waveguides and directional, To begin with, the SiOC coating depositions and characterizations is talked about that is trailed by the models of group for instance effectives indexes record as an element of waveguides width and its height. In advance, detached directional couplers are examined and the model that would be parametrized concerning the coupler's coefficient, the width of the waveguide, gaps between coupling is proposed.

2.1 SiOC Based waveguides

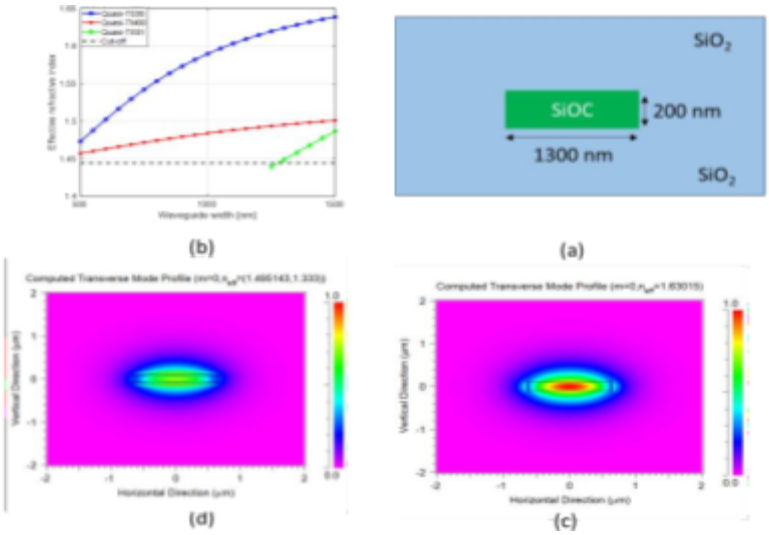

Fig. 1(a) The view of Cross-section of used silicon oxy carbide in an insulator waveguide. (b)For the thickness of 200 nm, SIOC waveguides and its effective index modes contrasted with the width of the waveguide as well as the index of the SiOC waveguide that is used in the simulation. SiOC waveguide and its profile of fields with the dimensions is calculated 1300 × 200 nm2 for field profile of SiOC waveguide (c) the mode of transverse electromagnetic (d) the mode of transverse magnetic.

Currently, optical properties as well as ratio (n) and constant of extinction (k) that was calculated with different angles spectroscopically and ellipsometry in a greater wavelength differ from three 300 nm till 1600 nm. There is high clearness in the SiOC film within the near-infrared region because it is about 10^{-4} higher than 800 nm in the annihilation constant. This cross-sectional image is placed in a SiOC film with a width of two hundred nm. Fig. 1(a) The SiOC waveguide's cross-section with given thickness height = 200 nm and width = 1300 nm. It seated the waveguide of 8 µm on top and the layer of buried oxide having a 4 micrometer thickness index cladding matched with the top oxide. The plasma and reactive gases Argon (Ar) and oxygen (O2) were utilized in the chamber of spluttering. Flow controller's mass and the rate in the flow of Argon and O2 gases were setup at the 15 cm and 0.5 cm along with the 350 W of RF power. To accomplish the vacuum condition high & impurities free, the

ISSN: 2446-2918 DOI: 10.21058/gjecs.20201.61001

mentioned pressure within the base given chamber was set to pumped down at 9 × 10^{-6} bar. Under these circumstances, the deposition rate was 10 nanometer/minute. The silicon substrate deposited with 8 micrometer the SiOC film and thermal oxide layer for 1200 seconds were set to be deposited in which 200 nm wideness was found. The waveguide performs as a multimode, and aspect of the waveguide rise consequently, to obtain the cut- off dimensions it is significant in which this waveguide performs as a single-mode waveguide. TE and TM modes in Fig. 1(b), and width will be fixed from 500 nm to 1500 nm waveguide for SiOC and a secure height of 200 nm. Meanwhile for the multiple layers of the waveguide silica (n = 1.444 at wavelength = 1550) is utilized, therefore, SiOC waveguide is measured as the cut-off effective index for the 1.444. Above the width of 1350 nm, the first higher-order TE mode the waveguide performs as a multimode start to broadcast. Therefore, the measured waveguide dimension is 1300 × 200 nm2 assumed as a standard single-mode whenever the refractive index is n = 2.2 at λ = 1550 nm for the SiOC waveguide. Secondly, no greater order Transverse Magnetic approach be located observed in any waveguide width. The SiOC waveguide for field profile of dimension is almost calculated as 1300 × 200 nm2 for the two different modes TE and TM as seen one-to-one in Figure. 1(c) and Figure. 1(d).

2.2 Mathematical Modelling

In Fig. 2 demonstrates the beneficial index or group indexes replications as just a feature of wide range for both the height 200 nm to plan a numerical mode for efficient indexes and group indexes of the SiOC waveguide which might function as a key component for path and probabilistic simulations. Figure 2(b) shows scientific results for group indexes for dual widths of waveguides. For both the group indexes of SiOC waveguides, the findings demonstrate broad consensus between both the predicted and measured data.

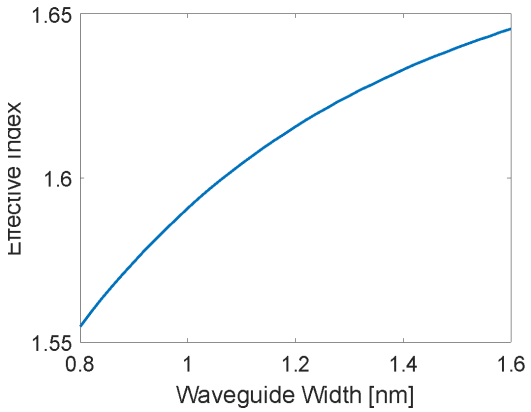

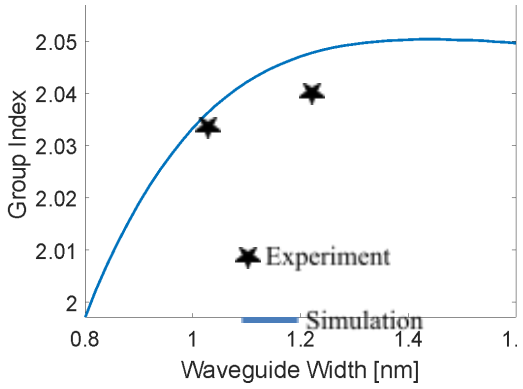

Fig. 2: (a) The effective index and (b) the group index as a function of waveguide width for the height 200 nm. Group index experimentally shown in waveguide width mentioned is1100 nm and 1300 nm.

In the mentioned model both effective and group indexes are considered as the function of the width of waveguides at the specific height h = 200 nm, showing in Fig. 4 (c), is assumed by (1) and (2), individually.

$$n_{eff} = a_1 w^3 + a_2 w^2 + a_3 w^1 + a_4 \qquad (1)$$

$$n_g = b_1 w^4 + b_2 w^3 + b_3 w^2 + b_4 w + b_5 \qquad (2)$$

Where, w is the waveguide width in nm, a_n and b_n are the constants with

$$a_1 = 5.751\times10^{-11}, a_2 = -3.097\times10^{-7}, a_3 = 0.0005989, a_4 = 1.243$$

$$b_1 = -4.47\times10^{-13}, b_2 = 2.364\times10^{-9}, b_3 = -4.745\times10^{-6}, b_4 = 0.004296,$$

$$b_5 = 0.5697$$

3. SiOC Based Directional Coupler.

The essential components that mostly used in the photonics' s field is Integrated directional coupler (DC) that is extensively utilize in multiple PICs likewise Mach-Zehnder interferometers (MZIs) as well as the ring resonators in optical switches application, optical splitter and polarization splitter. The two equivalent waveguides in predictable DC include the ratio of splitting amongst these dual waveguides for the measurement of the waveguides cavity and waveguide's coupler length.

The development in the microfabrication is typically used in the DC constructions in which the is constant g = 1000 nm and the of Lc = 176 μm and Lc = 356 μm two dissimilar lengths and the coefficient of coupling is fixed separately that is 0.5 and 1 (Showing in Fig. 3(a) in the point of the experiment. The dimensions set up 1300 × 200 nm^2 in the waveguide of the directional coupler. The power for the input is defined to the DC to split between the powers of its o/p i.e. *Po1* and *Po2*, it depends on the gap and coupling among the waveguides. The directional coupler coefficient coupling is specified by [14]:

$$k = sin\left(L_c \frac{\pi\Delta n}{\lambda^\circ}\right)^2 \qquad (3)$$

Where $\Delta n = neffe - neff$ variance of the real index for effective odd and even catalogues that depends upon the dimensions of the waveguide, and slit among the dual similar waveguides, and stays the essential wavelength. The term of (3) monitors an exponential presentation .Consequently in order to shorten the model of combination coefficient, the basic prototype for the future to compute coupling coefficient (K) coupling gap (g), coupling length (Lc) and waveguide width (w). The proposed formulation for the coefficient coupling is specified as:

ISSN: 2446-2918 DOI: 10.21058/gjecs.20201.61001

$$k = \sin sin\,(ae^{\gamma.\delta}L_c)^2 \quad (4)$$

In which, $a = 0.6219w2 - 2064w + 1.936 \times 106$ and $\gamma = 1.363 \times 10{-}9w2 - 4.281 \times 10{-}6w - 0.0009543$ and the arbitrary constants mostly depends upon the waveguide width of the waveguide in a certain constant height h = 200nm. The equations of the arbitrary constant are only valid when the gap between slits ranging from 500nm to 1200nm and their thickness h = 200 nm.

The waveguides dimensions 1300 × 200 nm^2 mentioned is in below Fig. 3 is obtained by the results of simulation and experimental methodologies the coupling length and for coupling gap g = 1000nm is the stimulated coupling coefficient. Although these coupling coefficient as shown in Fig. 3 (b) is considered as the function of Lc = 176μm coupling length and the coupling gap in addition two below Fig. 3 (a) and Fig. 3(b) showing a dotted line is basically the point of experimental data in the fabricated DC. We can also observe that these results obtained from experiments are synchronized with the simulations. In the below Eq. (4) the calculated mathematical model can also be utilized as a DC for any waveguides within a width range between 800nm to 1300nm.

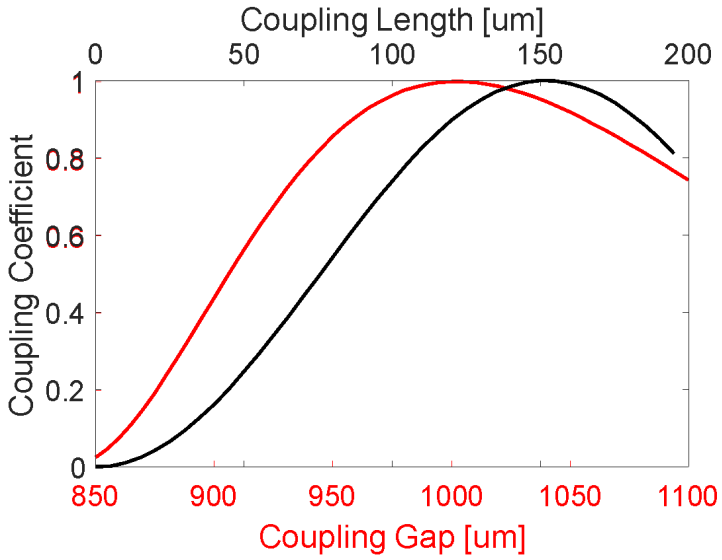

Fig. 3. Coupling coefficient as a function of coupling length at a gap of g = 800 nm (black line) and coupling gap (red line) for a constant coupling length of Lc = 356 μm.

4. Stochastic Simulation

The circuit simulators that mostly used commercially these equations, i.e. (1) – (3) modified BBs additionally utilize simulations on circuits. These BBs are calculated and oppressed to examine the performance in the photonic circuits. Using scattering

matrix formulas, each separated building block's considered that controlled authorization to perform simulations in the circuits. By means of that results that were reported in the preceding section found to be similar waveguide of the analytical prototype also the BBs of the multi-directional couplers. We also deliberate on the 5th order filter-based Mach Zehnder Interferometer (MZI) filter that completely relies on SiOC. The 5th order Mach-Zehnder filter is insignificant. Diagrammatically in Fig. 4(a), showing is found to be the synthesis technique that further is described.

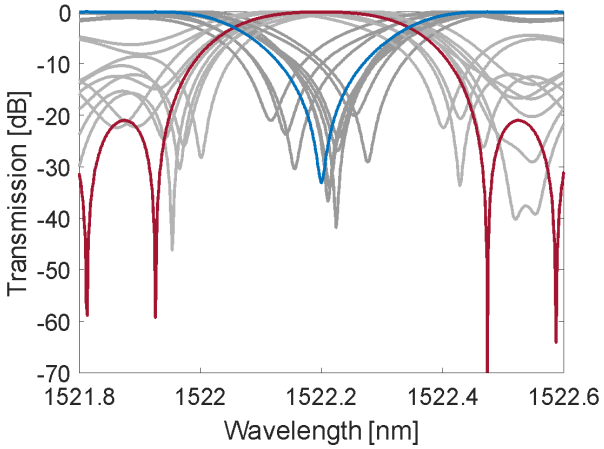

Fig. 4: Bar (red line) and Cross (blue line) ports of idea transfer function of 5th order Mach-Zehnder filter. Thin grey line shows the distorted transfer function due to stochastic uncertainties.

The Bandwidth of the MZI filter is almost 3 dB of, the coupling is parallel and its coefficient with the almost six couplers ranging from are K1 = K6 = 0.993, K2 = K5 =0.03 and K3 = K4 = 0.421 And its isolation in the in-band should be greater than the mentioned 30 Db all the six multidirectional couplers gi = 1 µm considered the couple length L1 = L6 = 333.9 µm. L2 = L5 = 39.1 µm and L3 = L4 = 158.5 µm. Prominent to the similar technology Wi = 1300 nm (i = 1 to 5) and height h = 200 nm of the waveguides as well as 1.6245 and 2.0525 [shown (1) and (2), and Fig. 2] is group and effective indices. The imbalance length is about 1460 µm in all the different five stages with 100 GHz of free spectral range (FSR) in addition to the transfer function in the MZI filter at two different ports (bold black) and (bold blue) respectively. These spectral responses do not reflect the inevitable variations process upsetting actual contrived circuits.

The stochastic analysis of the uncertainty and width of the waveguide and gaps between these two expected to be eliminated the dispersed arbitrary variables along with the standardized deviation In the shown Figure 5(b), the insignificant reactions in addition, several transfer spectral functions and cross ports of the MZI the filter is to be found by using…analyzation It realized obviously using the transfer functions of

unique design and it basically it will misrepresentative the case of measured negligible uncertainties and fluctuate both in-band and passband isolation.

Under the different fabrications, the compassion in the circuit is validated by using SiOC material and probability density function (PDF) of dissimilar interest secured gladly by using samples of 10^4 MC. The merging effects are to be a safeguard from the selected sample sizes. The PDF greatness in Fig. 5 showing at cross port and the wavelength is focused at 1522.3 nm. The irregular behavior noted for both different port. The massive deviation in the range of -40 to 0 dB at the cross port of the filter at a certain wavelength. The intensity found from a bigger deviation.

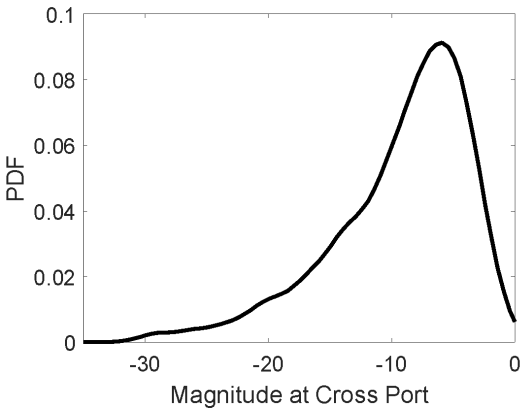

Fig. 5. PDF of magnitude variation of at the bar port of the filter at the 1550.2 nm central wavelengths. The PDF is obtained using the 10^4 samples using classical Monte Carlo technique.

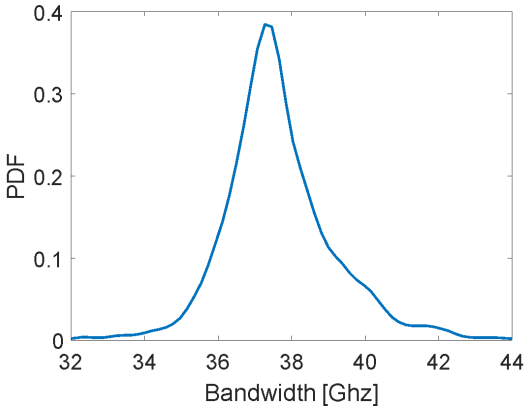

Fig. 6. PDF of 3 dB bandwidth at the bar port of the filter. The PDF is obtained using the 10^4 samples using classical Monte Carlo technique.

5. Conclusion

In this paper, we elaborate on the methodology and experimental limitations of the devices that relied on the SiOC likewise directional couplers and the waveguides. We also discoursed in this paper the Stochastic and circuits simulation relied on SiOC Technology. The SiOC depends on waveguides that are equipped physically BB's comprising the group and actual indexes, The losses caused due to width and heights were experimentally recognized by using its measuring data. We also established the prototype established on the building block directional couplers with the divergence of coupling gaps & coupling coefficient although waveguide width and it's coupling length in which the height of 220 nm is constant. The waveguides magnitude is set at 1300×200 nm^2 and the gap between 1000 nm its diverse pair of length and waveguide coefficient waveguides. The polarization coupling and its backscattering & sensitivity of polarization does not consist of building blocks and its on-going activity. In addition, The obtained results recognized the simulations on the circuits to

examine inconsistency in the stochastic process of the PICs design on the SiOC optimization to achieve its higher efficiency.

References

[1] Avgerou, M. Smit *et al.*, 'An introduction to InP-based generic integration technology', *Semicond. Sci. Technol.*, vol. 29, no. 8, p. 083001, Jun. 2014.

[2] D. Melati *et al.*, 'Validation of the Building-Block-Based Approach for the Design of Photonic Integrated Circuits', *J. Light. Technol.*, vol. 30, no. 23, pp. 3610–3616, Dec. 2012.

[3] M. Hochberg and T. Baehr-Jones, 'Towards fabless silicon photonics', *Nat. Photonics*, vol. 4, no. 8, pp. 492–494, Aug. 2010.

[4] T. Korthorst, R. Stoffer, and A. Bakker, 'Photonic IC design software and process design kits', *Adv. Opt. Technol.*, vol. 4, no. 2, Jan. 2015.

[5] X. J. M. Leijtens, P. Le Lourec, and M. K. Smit, 'S-matrix oriented CAD-tool for simulating complex integrated optical circuits', *IEEE J. Sel. Top. Quantum Electron.*, vol. 2, no. 2, pp. 257–262, Jun. 1996.

[6] L. David, R. Bhandavat, U. Barrera, and G. Singh, 'Silicon oxycarbide glass-graphene composite paper electrode for long-cycle lithium-ion batteries', *Nat. Commun.*, vol. 7, no. 1, p. 10998, Apr. 2016.

[7] V. S. Pradeep, M. Graczyk-Zajac, R. Riedel, and G. D. Soraru, 'New Insights in to the Lithium Storage Mechanism in Polymer Derived SiOC Anode Materials', *Electrochim. Acta*, vol. 119, pp. 78–85, Feb. 2014.

[8] A. Grill, 'Plasma enhanced chemical vapor deposited SiCOH dielectrics: from low- k to extreme low- k

[9] H. J. Kim, Q. Shao, and Y.-H. Kim, 'Characterization of low-dielectric-constant SiOC thin films deposited by PECVD for interlayer dielectrics of multilevel interconnection', *Surf. Coatings Technol.*, vol. 171, no. 1–3, pp. 39–45, Jul. 2003.

[10] M. R. Wang, Rusli, J. L. Xie, N. Babu, C. Y. Li, and K. Rakesh, 'Study of oxygen influences on carbon doped silicon oxide low k thin films deposited by plasma enhanced chemical vapor deposition', *J. Appl. Phys.*, vol. 96, no. 1, pp. 829–834, Jul. 2004.

[11] V. Nikas *et al.*, 'The origin of white luminescence from silicon oxycarbide thin films', *Appl. Phys. Lett.*, vol. 104, no. 6, p. 061906, Feb. 2014.

[12] A. Karakuscu, R. Guider, L. Pavesi, and G. D. SorarÃ1, 'White Luminescence from Solâ€“Gel-Derived SiOC Thin Films', *J. Am. Ceram. Soc.*, vol. 92, no. 12, pp. 2969–2974, Dec. 2009.

[13] Y. PENG, J. ZHOU, X. ZHENG, B. ZHAO, and X. TAN, 'STRUCTURE AND PHOTOLUMINESCENCE PROPERTIES OF SILICON OXYCARBIDE THIN FILMS DEPOSITED BY THE RF REACTIVE SPUTTERING', *Int. J. Mod. Phys. B*, vol. 25, no. 22, pp. 2983–2990, Sep. 2011.

[14] Y. Ding, H. Shirai, and D. He, 'White light emission and electrical properties of silicon oxycarbide-based metal–oxide–semiconductor diode', *Thin Solid Films*, vol. 519, no. 8, pp. 2513–2515, Feb. 2011.

[15] G. Bellocchi, G. Franzò, M. Miritello, and F. Iacona, 'White light emission from Eu-doped SiOC films'.

[16] Waqas, A., Memon, F. A., & Korai, U. A. (2020). Experimental validation of a building block of passive devices and stochastic analysis of PICs based on SiOC technology. Optics Express, 28(15), 21420-21431.

[17] A. Waqas, D. Melati, and A. Melloni, 'Sensitivity Analysis and Uncertainty Mitigation of Photonic Integrated Circuits', *J. Light. Technol.*, vol. 35, no. 17, pp. 3713–3721, Sep. 2017.

[18] D. Melati, A. Waqas, and A. Melloni, 'Stocastic photonics: Tools and approaches for the analysis and optimization of integrated circuits', in *2017 Opto-Electronics and Communications Conference (OECC) and Photonics Global Conference (PGC)*, 2017, pp. 1–3.

[19] A. Waqas, D. Melati, and A. Melloni, 'Stochastic simulation and sensitivity analysis of photonic circuit through Morris and Sobol method', in *Optical Fiber Communication Conference*, 2017, p. Th2A.3.

[20] X. Chen, M. Mohamed, Z. Li, L. Shang, and A. R. Mickelson, 'Process variation in silicon photonic devices', *Appl. Opt.*, vol. 52, no. 31, p. 7638, Nov. 2013.

[21] A. Waqas, D. Melati, B. S. Chowdhry, and A. Melloni, 'Efficient Variability Analysis of Photonic Circuits by Stochastic Parametric Building Blocks', *IEEE J. Sel. Top. Quantum Electron.*, vol. 26, no. 2, pp. 1–8, Mar. 2020.

[22] A. Waqas, D. Melati, P. Manfredi, and A. Melloni, 'Stochastic process design kits for photonic circuits based on polynomial chaos augmented macro-modelling', *Opt. Express*, vol. 26, no. 5, p. 5894, Mar. 2018.